Thin Solid Films 519 (2010) 880–884

Contents lists available at ScienceDirect

Thin Solid Films

journal homepage: www.elsevier.com/locate/tsf

Hydrogen gas sensing performance of Pd–Ni alloy thin films

Eunsongyi Lee [a,1], Jun Min Lee [a,1], Eunyoung Lee [a], Jin-Seo Noh [a], Jin Hyoun Joe [a], Bumsuk Jung [b], Wooyoung Lee [a,*]

[a] Department of Materials Science and Engineering, Yonsei University, 262 Seongsanno Seodaemun-gu, Seoul, 120-749, Korea
[b] Department of Environmental Engineering and Biotechnology, Myongji University, San 38-2 Nam-dong, Yongin, Kyunggi-do, 449-728, Korea

ARTICLE INFO

Article history:
Received 16 February 2010
Received in revised form 23 July 2010
Accepted 29 July 2010
Available online 4 August 2010

Keywords:
Palladium (Pd)
Nickel (Ni)
Pd–Ni alloy thin film
Hydrogen gas
Phase transition

ABSTRACT

We investigated the hydrogen (H_2) sensing properties of palladium (Pd)–nickel (Ni) alloy films with varying Ni content and discussed them in light of structural deformations. The Pd–Ni alloys operated reversibly upon H_2 absorption and desorption and their sensitivities decreased linearly with Ni content added to Pd. This was attributed to reduction in the lattice constant and interstitial volume caused by the Ni addition, allowing fewer hydrogen atoms to penetrate into the Pd–Ni alloy with higher Ni content. Interestingly, the response time of the Pd–Ni alloys was much shorter than that of pure Pd, presumably due to the fast permeation of hydrogen atoms through microscopic imperfections in the alloys. Unlike pure Pd, the Pd–Ni alloys showed an almost linear relationship between the sensitivity and H_2 concentration without hysteretic behaviors, enabling the detection of low concentration of H_2 down to 0.01%. These results provide a significant understanding of the role of Ni in the Pd–Ni thin films for improving the H_2 sensing properties of the Pd-based alloy film sensors.

1. Introduction

In recent years, hydrogen (H_2) has gained much interest as a potential energy source because of its important attributes such as renewability, abundance, and efficiency [1,2]. Hydrogen, however, is flammable and explosive when its concentration exceeds 4% in air [3]. Hence, immediate detection of hydrogen is extremely important over a wide range of concentrations. Many researches have focused on the development of hydrogen sensing materials with high sensitivity and reliability. Commercialized hydrogen sensors can be generally divided into two types, the hot wire type [4] and the electrochemical type [5]. However, these sensors have critical problems such as high power consumption, high operating temperature, and poor hydrogen selectivity.

Another type of hydrogen sensor is the metal oxide semiconductor sensor, which can detect low concentrations of hydrogen gas [6,7]. This sensor, however, showed premature saturation in detectable hydrogen concentrations, along with other drawbacks such as low sensitivity and high power consumption. Over the past few decades, use of Pd as a hydrogen sensor material has attracted much attention because of its high sensitivity to hydrogen [8–14]. Palladium has been incorporated into nano-wires [9,10], nano-tubes [11,12], and nano-chains [13,14] to reduce size, decrease power consumption, and enhance sensing properties. Despite the superior sensitivity of Pd-based hydrogen sensors, they have several drawbacks. For example, volume expansion by hydrogen absorption causes changes in the structure of Pd thin films and results in hysteresis behavior in electrical resistance [8,15]. To improve the structural stability, Pd alloy thin films [16] have been investigated such as Pd–Mg [17], Pd–Au [18], Pd–Ag [19], and Pd–Ni [20,21] alloys. Among these candidates, the Pd–Ni alloy has been spotlighted due to its durability and fast response.

In this study, we have investigated the changes in lattice structure and hydrogen sensing properties of Pd–Ni alloys as a function of Ni concentration. In addition, phase transitions were investigated for pure Pd and Pd–Ni alloy thin films and linear response behaviors of the Pd–Ni alloys were discussed in association with suppression of phase transitions in those alloys. Finally, we have determined the optimal Ni concentration to achieve high sensing properties in the Pd–Ni alloy thin films.

2. Experiments

Pd–Ni alloy thin films were deposited onto thermally oxidized Si (100) substrates by an ultra-high vacuum DC magnetron co-sputtering (base pressure = 5.3×10^{-6} Pa (4×10^{-8} Torr), working pressure = 0.24 Pa (1.8×10^{-3} Torr)) at room temperature, using pure palladium (Pd, 99.99% purity) and pure nickel (Ni, 99.99% purity) targets. By adjusting the power applied to the Pd and Ni targets, the ratios of Pd to Ni in the alloy films were controlled. Six types of Pd–Ni alloy thin films were fabricated with different Ni ratios (Ni/Pd = 0%, 4%, 7%, 10.5%, 12.4%, 20% and 26%). The thicknesses of the

* Corresponding author. Tel.: +82 2 2123 2834; fax: +82 2 312 5375.
E-mail address: wooyoung@yonsei.ac.kr (W. Lee).
[1] These authors equally contributed to this work.

0040-6090/$ – see front matter © 2010 Elsevier B.V. All rights reserved.
doi:10.1016/j.tsf.2010.07.122

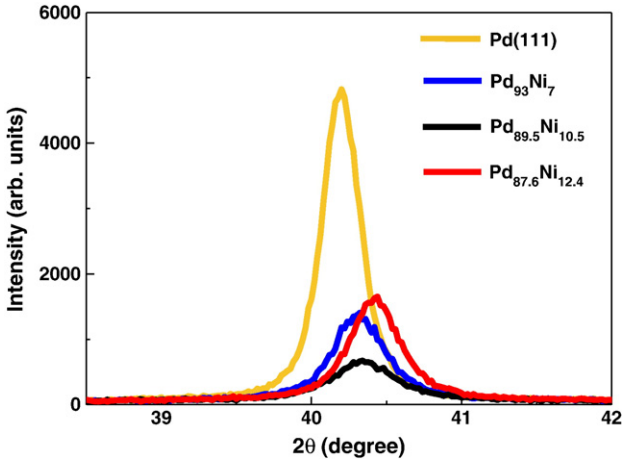

Fig. 1. The θ–2θ X-ray diffraction patterns of thin films of pure Pd, $Pd_{93}Ni_7$, $Pd_{90}Ni_{10}$, and $Pd_{88}Ni_{12}$.

Pd–Ni alloy films varied from 5 to 400 nm. To measure their electric properties, all samples were wired using a wire bonder. The measurement system consisted of a sealed chamber (250 mL) with a gas inlet and outlet, mass flow controllers for monitoring the ratio of H_2 to N_2, and digital multimeters connected to a personal computer. Two gases from different lines were mixed beforehand, flowing into the chamber through the gas inlet line. The pressure in the chamber was maintained at near atmospheric pressure. The Pd–Ni alloy sensors were used to detect H_2 in the concentration range of 0.01–10% at room temperature by measuring changes in their electrical resistances. All data acquisition was performed with a National Instruments LabView program through a General Purpose Interface Bus. The formation of solid solution crystals was investigated using X-ray diffraction (XRD), and the ratios of Pd to Ni in the alloy thin films were measured with an energy dispersive X-ray spectrometer. In addition, the surface morphologies of the samples were observed using a confocal laser scanning microscopy.

3. Results and discussion

The lattice constants of Pd and Ni are 3.891 Å and 3.524 Å, respectively [22]. When compared with that of Pd, the lattice constant of Ni is 10% lower, and they both have an FCC lattice structure. From a structural perspective, one expects the formation of a substitutional solid solution between the two pure metals. Nickel diffuses into Pd and can substitute for Pd. Compared with Pd, the lattice constant of a Pd–Ni alloy is smaller due to the influence of the added Ni, leading to smaller volume in each interstitial site. The formation of solid solution crystals can be confirmed from the XRD patterns shown in Fig. 1, which correspond to (111) peaks. The XRD patterns of the Pd–Ni alloy films were obtained from alloys including 7, 10.5, and 12.4% Ni contents, respectively. The 2θ values of the Pd–Ni alloys are higher compared with that of pure Pd, indicating that the lattice constants of the alloys are smaller than pure Pd, as mentioned above. The peak

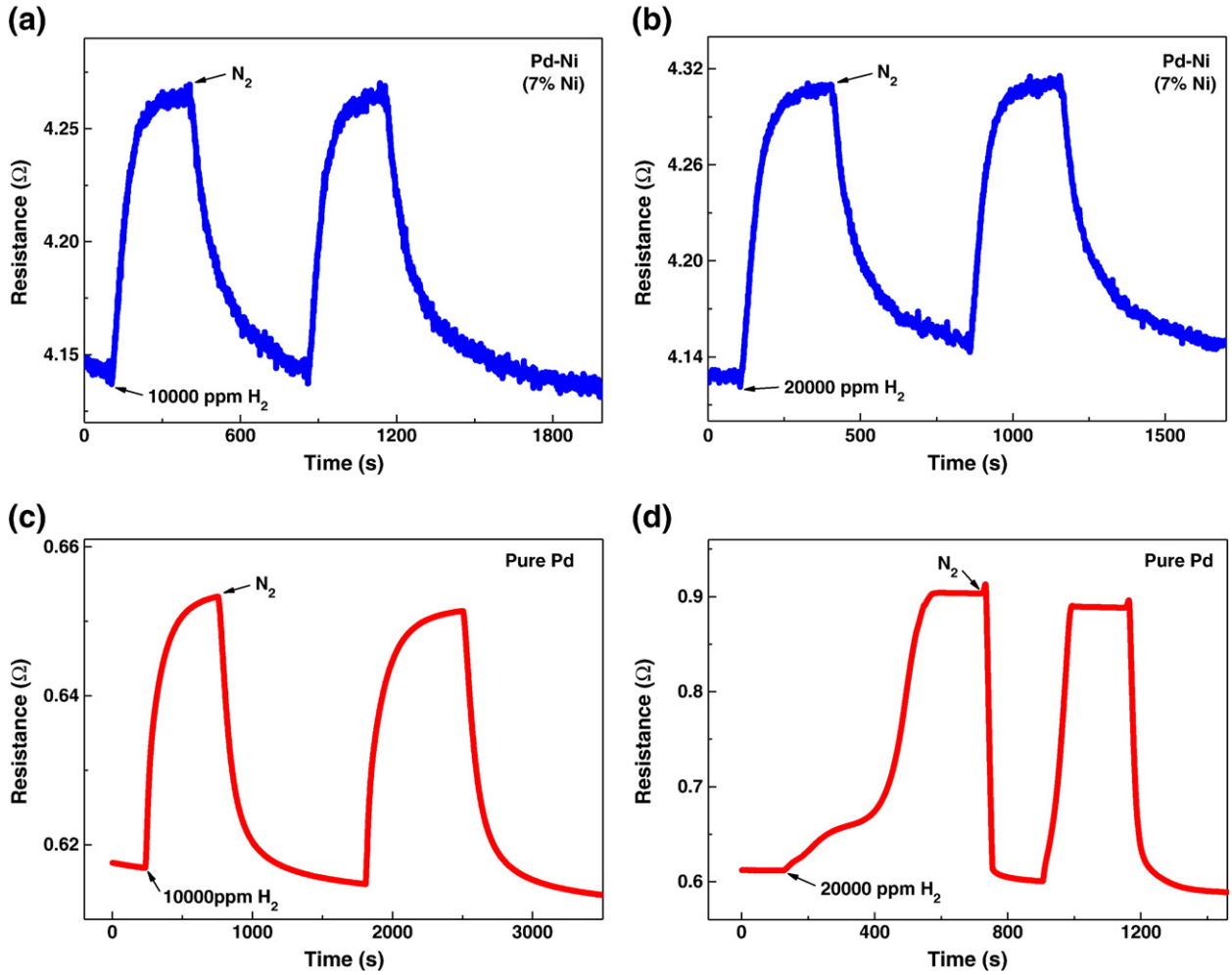

Fig. 2. Plots of real-time electrical resistance responses after exposure to 1% and 2% H_2 for pure Pd ((a), (b)) and Pd–Ni (7% Ni) alloy sensors ((c), (d)), respectively, at room temperature.

positions are gradually shifted to higher values with increasing Ni concentration in the Pd–Ni alloys, confirming a gradual decrease in the lattice constant due to the increasing contribution of Ni. In addition, the full width at half maximum of the Pd–Ni alloys is larger as compared to that of pure Pd, reflecting that the solid solutions are less perfect in crystallinity, presumably because they contain many imperfections such as grain boundaries and dislocations to compensate for the lattice mismatch between Pd and Ni. The reduction in lattice constant and increase in imperfections in the Pd–Ni alloys are related to the sensitivity and response time of the materials, as described in the following paragraphs.

The fundamental operation principles of Pd–Ni alloys are based on changes in their resistance upon H_2 absorption/desorption, resulting in the ability to operate at sufficiently low temperatures. To measure the variations in their electrical resistances with gas absorption and desorption, each thin film was first exposed to N_2 to obtain a baseline, then to a designated concentration of H_2, and then back to N_2, thus completing one cycle. Fig. 2 illustrates the representative electrical resistances after exposure to 1 and 2% H_2 for pure Pd and Pd–Ni (7%) alloy sensors. Fig. 2(a) and (c) shows comparative changes in the resistance of pure Pd and a Pd–Ni alloy upon exposure to 1% H_2. The increase in the resistances of the samples can be attributed to increased scattering due to the incorporation of H atoms in the interstitial sites of the Pd–H system. The sensitivity of the films to H_2 is defined as

$$\text{Sensitivity}\ (\%) = \frac{R_H - R_N}{R_N} \times 100,$$

where R_H and R_N are the resistances in the presence of H_2 and N_2 gases, respectively. The sensitivities of pure Pd and Pd–Ni (7% Ni) were 5.1% and 3.1%, respectively. Response time is defined as the time required to reach 36.8% ($=e^{-1}$) of the total change in the electric resistance at a given H_2 concentration. The response times of pure Pd and Pd–Ni (7% Ni) were 49 sec and 5 sec, respectively. When compared with pure Pd, the response time of the Pd–Ni alloy was almost 10 times smaller. Fig. 2(b) and (d) illustrates relative changes in the resistance of pure Pd and Pd–Ni alloy, respectively, upon exposure to 2% H_2. When the pure Pd thin film in the presence of H_2 is considered, the H_2 molecules are decomposed into single H atoms, and they are absorbed in the interstitial sites of the Pd lattice through a diffusion process to form a solid solution of Pd–H (α-phase) at low hydrogen concentration and a hydride (β-phase) at high hydrogen concentration. In the Pd–H system, the α-phase and β-phase can be obtained depending on the amount of H atoms incorporated into the Pd thin films. The phase transition from α- to β-phase occurs during the absorption process of H atoms, if the amount of incorporated H atoms exceeds the maximum H solid solubility in the Pd film [8,23]. During the increments of the first cycle, an intermediate stage shown as a plateau region was observed from 250 sec to 375 sec, followed by a further increase in the resistance values. This behavior can be attributed to the phase transition of the Pd thin film from the α- to β-phase. In addition, when exposed to 2% H_2, the increase in resistance of the Pd thin film was probably due to increased carrier scattering, owing to an excess of incorporated H atoms and additional defects such as vacancies and dislocations formed during the delamination process of the Pd surface [24]. The structural deformation of the Pd thin film, which occurred during the phase transition from the α- to β-phase, was primarily due to numerous H atoms diffusing into the Pd film, wherein significant numbers of H atoms broke bonds of the Pd system. In the case of the Pd–Ni alloys, however, the point of inflection was not observed for H_2 exposures below 2%.

The occurrence of phase transitions can also be identified by surface delamination. The surface change of thin films upon H_2 exposure was investigated using confocal laser scanning microscopy (CLSM). Fig. 3 shows CLSM images of pure Pd and Pd–Ni (4% Ni) alloy thin films after exposure to 2% H_2. The CLSM image of the surface of the pure Pd thin film clearly shows surface delamination, as seen in Fig. 3(a). The surface delamination originates from the volume expansion of the film during phase transition, which generates tensile stress at the interface between the film and substrate, and the subsequent structural deformation of the film to relieve this stored stress [25–27]. The structural deformation in the Pd film was irreversible, and the deformed structure remained unchanged even after the H atoms were desorbed from the hydrogenated Pd. In contrast, the surface of the Pd–Ni (4% Ni) alloy thin film contains no significant defects, as shown in Fig. 3(b). This clean surface morphology of the alloy film suggests that any macroscopic structural deformation, in turn, a massive phase transition did not occur when the film was exposed to H_2. The suppression of the phase transition by the addition of Ni is reasonable because the Pd–Ni alloy can accommodate fewer H atoms due to the reduced interstitial volume, and H atoms may preferentially permeate through imperfections like grain boundaries and dislocations, as discussed above.

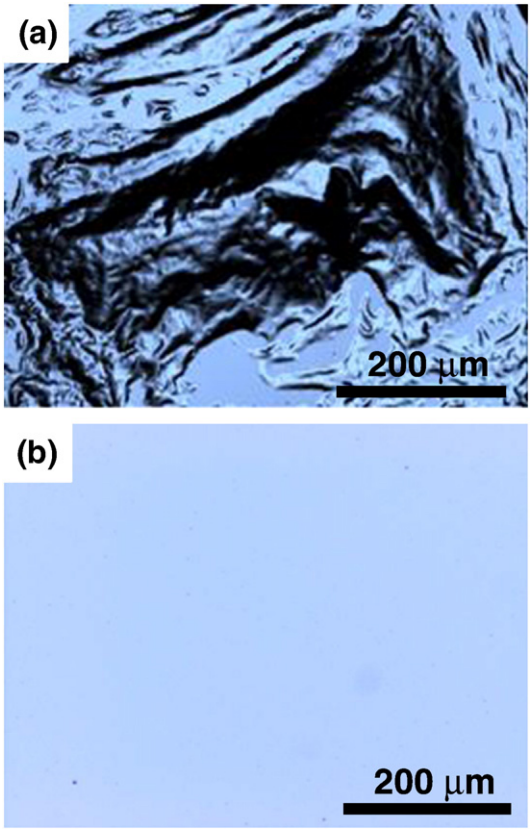

Fig. 3. Confocal laser scanning microscopy images of the surface of (a) thin Pd film and (b) Pd–Ni alloy thin film after exposure to 2% H_2.

Fig. 4 illustrates plots of the sensitivity and response time of the Pd–Ni alloy sensors as a function of Ni content upon exposure to 1% H_2, compared with those of the pure Pd sensor. With increasing Ni concentration, the amplitude of the sensitivity decreases, but the response time improves dramatically until Ni content reaches 7%. In the case of the Pd–Ni alloy, the β-phase is not formed in the measured H_2 concentration range in accordance with the prior study [28]. Consequently, the electrical resistance of Pd–Ni alloy films increases linearly with increasing hydrogen concentration in the original β-phase region. Moreover, the addition of Ni to the Pd matrix reduces the probability that hydrogen atoms penetrate into the thin films due to the reduced interatomic distance and interstitial volume. It is similar to the case of reducing film thickness. Under this circumstance, the sensitivity of the sensor decreases as a function of Ni content added to Pd, as demonstrated in Fig. 4(a). In a similar

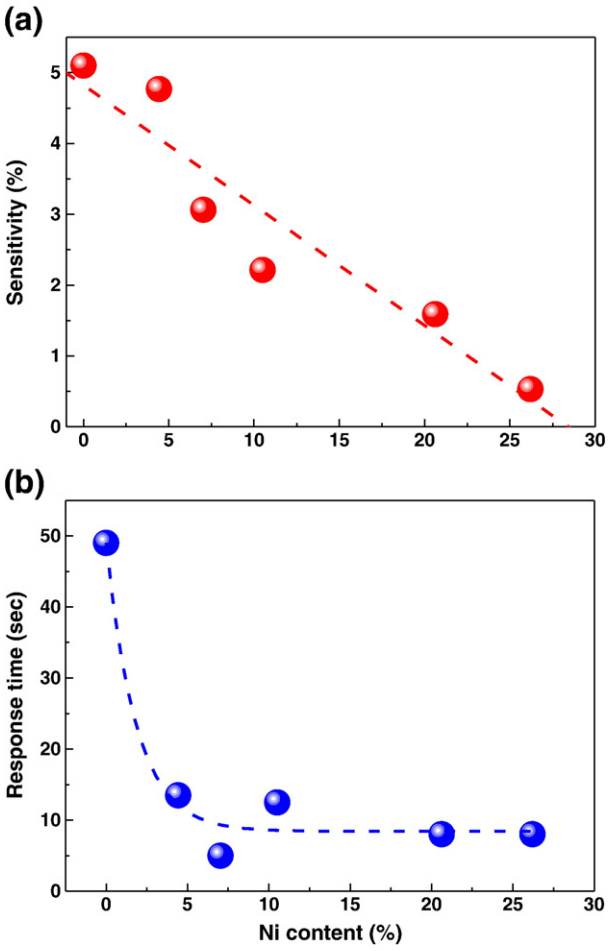

Fig. 4. Plots of (a) sensitivity and (b) response time to 1% H_2 as a function of Ni content in Pd–Ni alloy thin films.

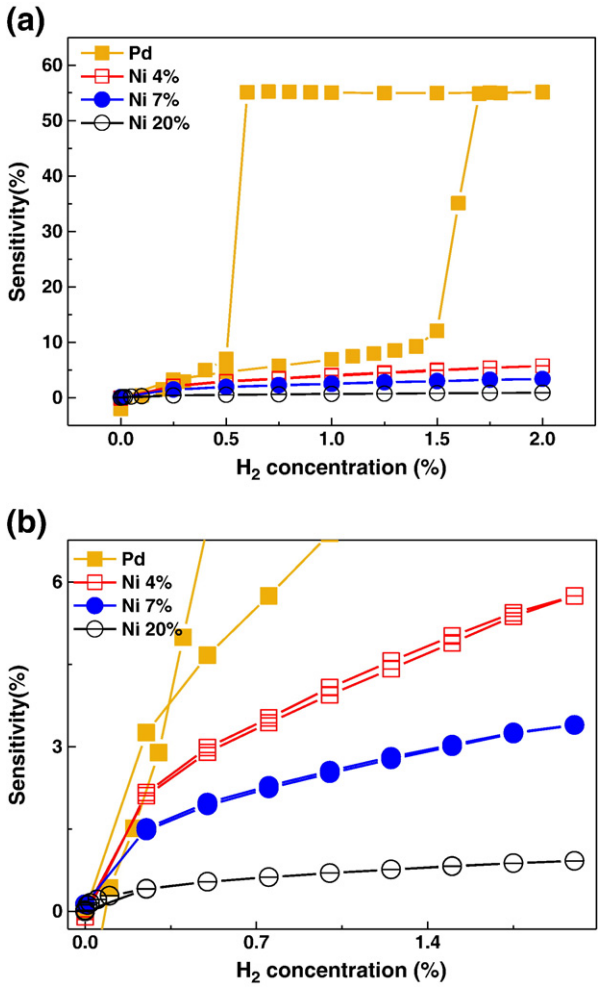

Fig. 5. Plot of (a) sensitivity as a function of H_2 concentration in the range of 0–2% for pure Pd, Pd–Ni (4% Ni), Pd–Ni (7% Ni), and Pd–Ni (20% Ni), respectively, (b) an enlarged plot of (a).

context, we believe that the rapid decrease in response time of the Pd–Ni alloy films may be caused by the addition of a small amount of Ni, since such imperfections as grain boundaries and dislocations formed to compensate for the lattice mismatch between Pd and Ni can quickly interact with H atoms. It is inferred that the imperfection density would reach a maximum at a certain level of Ni, and beyond that, additional Ni may degrade the grain quality. As a result, the first large decrease in the response time occurs within 7% Ni and then, the response time shows a weak dependence on Ni content until it is saturated. Based on the observed results, the Pd–Ni alloy sensors can effectively detect a wide range of H_2 concentrations within a short response time.

Fig. 5 shows changes in sensitivities of pure Pd and Pd–Ni alloy sensors as a function of H_2 concentration. To examine whether the phase transition occurs in the Pd–Ni alloy thin films, the Ni content was varied from 0 to 20% and the sensitivity behaviors of each thin film were investigated in an H_2 concentration range of 0 to 2%. As shown in Fig. 5, when exposed up to 2% H_2, there is a significant hysteresis behavior observed in the pure Pd sensor. During the phase transition from the α- to β-phase and back to the α-phase, the hysteresis in the resistance [8,15] is attributed to irreversible structural changes [25–28] in the Pd films. Additionally, it is observed that the pure Pd sensor has a maximum solid solubility of 1.5% H_2, and beyond that, the sensitivity rapidly increases due to the phase transition to the β-phase. In the case of Pd–Ni alloy sensors, on the other hand, no hysteresis behavior is observed during the absorption/desorption process for up to 2% H_2. In contrast to the pure Pd sensor, the Pd–Ni alloy sensors show an almost linear increase in sensitivity with H_2 concentrations up to 2%. In particular, the Pd–Ni (20% Ni) alloy sensor responded to very low concentrations (down to 0.01%) of H_2. Unfortunately, with increasing Ni concentration, there was no improvement in the sensitivity, as compared with that of the pure Pd sensor. Nevertheless, the good linearity in sensitivity and the short response time of the Pd–Ni alloy sensors make it possible to quickly detect hydrogen gas over a wide concentration range at room temperature.

4. Conclusions

We have fabricated highly sensitive hydrogen gas sensors based on Pd–Ni alloy thin films. The Pd–Ni alloy thin films were deposited on thermally oxidized Si (100) substrates by DC co-sputtering. X-ray diffraction (XRD) was used to analyze the changes in the lattice of the Pd–Ni alloys. It was found that the peak positions of the Pd–Ni alloys were shifted to higher values by the addition of Ni to Pd, indicating a gradual decrease in lattice constant. The structural deformation of the Pd–Ni alloy films corresponding to the phase transition from the α- to β-phase was effectively suppressed by the addition of Ni, while surface delamination was observed in the pure Pd films upon exposure to 2% H_2. The changes in electrical resistance of the Pd–Ni alloy sensors reversibly occur while undergoing H_2 absorption/desorption cycles, and their response time was much shorter than that of pure Pd. Unlike pure Pd, the Pd–Ni alloy sensors showed an almost linearly increasing response to H_2 concentration over the measured concentration range, which allowed for detection of low

concentrations (down to 0.01%) of H_2. The optimal Ni content was determined to be approximately 7% in Pd–Ni alloys. These results suggest that it is possible to fabricate highly sensitive H_2 sensors using Pd–Ni alloy thin films, which exhibit fast response and recovery.

Acknowledgments

This work was supported by Priority Research Centers Program (2009-0093823) through the National Research Foundation of Korea (NRF) and the Basic Research Program grant (2009-0083794).

References

[1] V.A. Goltsov, T.N. Veziroglu, L.F. Goltsova, Int. J. Hydrogen Energy 31 (2006) 153.
[2] S. Shukla, S. Seal, L. Ludwig, C. Parish, Sens. Actuators, B 97 (2004) 256.
[3] J.G. Firth, A. Jones, T.A. Jones, Combust. Flame 21 (1973) 303.
[4] A. Katsuki, K. Fukui, Sens. Actuators, B 52 (1998) 30.
[5] E. Bakker, M. Telting-Diaz, Anal. Chem. 74 (2002) 2781.
[6] K.I. Lundström, M.S. Shivaraman, C.M. Svensson, J. Appl. Phys. 46 (1975) 3876.
[7] B.S. Kang, F. Ren, B.P. Gila, C.R. Abernathy, S.J. Pearton, Appl. Phys. Lett. 84 (2004) 1123.
[8] F.A. Lewis, The Palladium Hydrogen System, Academic, New York, 1967.
[9] M.H. Yun, N.V. Myung, R.P. Vasquez, C. Lee, E. Menke, R.M. Penner, Nano Lett. 4 (2004) 419.
[10] Y.H. Im, C. Lee, R.P. Vasquez, M.A. Bangar, N.V. Myung, E.J. Menke, R.M. Penner, M.H. Yun, Small 2 (2006) 356.
[11] F. Favier, E.C. Walter, M.P. Zach, T. Benter, R.M. Penner, Science 293 (2001) 2227.
[12] M.Z. Atashbar, S. Singamaneni, Sens. Actuators, B 111 (2005) 13.
[13] J. Kong, M.G. Chapline, H. Dai, Adv. Mater. 13 (2001) 1384.
[14] Y. Sun, H.H. Wang, Appl. Phys. Lett. 90 (2007) 213.
[15] R.C. Hughes, W.K. Schubert, R.J. Buss, J. Electrochem. Soc. 142 (1995) 249.
[16] K. Baba, U. Miyagawa, K. Watanabe, Y. Sakamoto, T.B. Flanagan, J. Mater. Sci. 25 (1990) 3910.
[17] S. Nakano, S. Yamaura, S. Uchinashi, H. Kimura, A. Inoue, Sens. Actuators, B 104 (2005) 75.
[18] X.M.H. Huang, M. Manolidis, S.C. Jun, J. Hone, Appl. Phys. Lett. 86 (2005) 143104.
[19] M. Wang, Y. Feng, Sens. Actuators, B 123 (2007) 101.
[20] Y.-T. Cheng, Y. Li, D. Lisi, W.M. Wang, Sens. Actuators, B 30 (1996) 11.
[21] L. Huang, H. Gong, D. Peng, G. Meng, Thin Solid Films 345 (1999) 217.
[22] G.W. Watson, R.P.K. Wells, D.J. Willock, G.J. Hutchings, J. Phys. Chem. B 105 (2001) 4889.
[23] K.J. Jeon, M.H. Jeun, E.S.I. Lee, J.M. Lee, K.I. Lee, P. von Allmen, W.Y. Lee, Nanotechnology 19 (2008) 495501.
[24] Y. Sakamoto, I. Takashima, J. Phys. Condens. Matter 8 (1996) 10511.
[25] R.C. Hughes, W.K. Schubert, T.E. Zipperian, J.L. Rodriguez, T.A. Plut, J. Appl. Phys. 62 (1987) 1074.
[26] A. Othonos, K. Kalli, D.P. Tsaib, Appl. Surf. Sci. 161 (2000) 54.
[27] R. Dus, R. Nowakowski, E. Nowicka, J. Alloys Compd. 404 (2005) 284.
[28] M.V. Goltsova, Y.A. Artemenko, V. Zaitsev, J. Alloys Compd. 293 (1999) 379.